Ab Initio Molecular Orbital Study of the Electronic Structure and the Rotational Barrier of Benzene in the "Helicopter" Complex $Os_3(CO)_9(C_6H_6)$

Jean-Frédéric Riehl,† Nobuaki Koga,†,‡ and Keiji Morokuma*,†

Institute for Molecular Science, Myodaiji, Okazaki 444, Japan, College of General Education and Graduate School of Human Informatics, Nagoya University, Nagoya 464-01, Japan, and Cherry L. Emerson Center for Scientific Computation and Department of Chemistry, Emory University, Atlanta, Georgia 30322

Received July 2, 1993®

A theoretical analysis is presented on the structure, bonding nature, and rotational barrier of the $Os_3(CO)_9(C_6H_6)$ complex, which has a benzene molecule in a new face-capping μ_3-η^2:η^2:η^2 coordination mode. Using RHF geometry optimization and MP2 calculations, we have estimated the interaction energy between the $Os_3(CO)_9$ fragment and the benzene molecule, as well as the benzene rotational barrier with respect to the Os_3 triangle (15.9 kcal/mol). An MO analysis leads to an interpretation of the interaction between $Os_3(CO)_9$ and benzene in terms of donation and back-donation which are enhanced by the CH bending. The origin of the Kekulé distortion of benzene has been attributed to an increase in the back-donation and a decrease in exchange repulsion due to benzene π electrons. The rotational barrier is caused by a decrease in the back-donation and an increase in exchange repulsion due to benzene σ electrons. A comparison has been made among the interactions of this polymetallic compound with benzene and ethylene as well as those of a model monometallic fragment with ethylene and benzene.

Introduction

The chemistry of an arene ligand bonded to one or several metal centers has been the subject of a large number of experimental studies, the most commonly studied compounds being probably the ML_3–arene species or the sandwich complexes.[1] The high symmetry and large size of arene ligands give enough flexibility to find appropriate metal orbitals overlapping with its π and π^* orbitals and form stable complexes in a variety of coordination modes, from a highly symmetric η^6 coordination to low-symmetry modes such as η^4 (pseudodiene) or η^2 (pseudoolefin) (1).

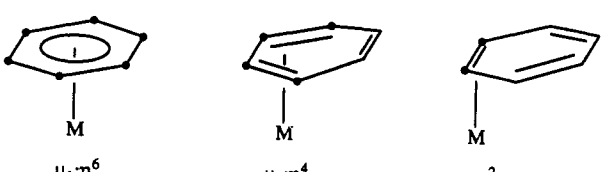

1

Most of the interactions of an arene with a single metal can be interpreted with the well-accepted donation–back-donation bonding scheme of Dewar–Chatt–Duncanson. In polymetallic systems, the most common case is an η^6-arene ligand bound to a single atom (μ_1-η^6), with geometrical parameters comparable to those of monometallic compounds. A different mode is obtained, however, when benzene reacts with some trinuclear clusters of osmium or ruthenium; a benzyne (C_6H_4) unit is coordinated to two metal centers via the two unsubstituted carbon atoms, the in-plane double bond between them interacting with the third metal atom (μ_3-η^2, 2). Because of the large variety of published data, this chemistry is today fairly well understood and both metal–carbon and carbon–carbon distances can be predicted with a good accuracy when a new complex is synthesized.[1,2]

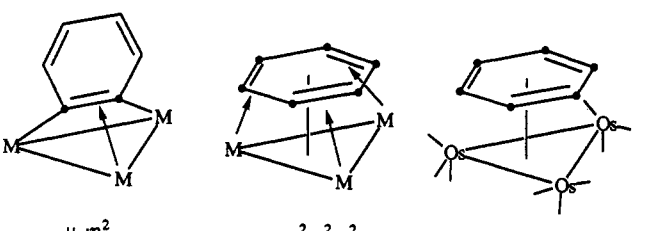

2 3 4

Recent studies have established a new face-capping bonding mode of benzene on the top of a trimetallic triangular face (μ_3-η^2:η^2:η^2 coordination, 3). The first examples were reported in 1985 by Johnson et al. with the trimetallic $Os_3(CO)_9(\mu_3$-η^2:η^2:η^2-$C_6H_6)$ (4) and hexametallic $Ru_6C(CO)_{11}(\eta^6$-$C_6H_6)(\mu_3$-η^2:η^2:η^2-$C_6H_6)$ clusters.[3] Since then, other compounds have been synthesized, involving trimetallic carbonyl clusters[4] or cyclopentadienyl clusters such as $(CoCp)_3(\mu_3$-$C_6H_5CH{=}CHMe)$[5] or $Ru_3Cp^*_3(\mu$-$H)_3$-

* To whom correspondence should be addressed at Emory University.
† Institute for Molecular Science.
‡ Nagoya University.
® Abstract published in *Advance ACS Abstracts,* October 15, 1993.

(1) (a) Mutterties, E. L.; Bleeke, J. R.; Wucherer, E. J.; Albright, T. A. *Chem. Rev.* **1982**, *82*, 499 and references therein. (b) Gastinger, R. D.; Klabunde, K. J. *Transition Met. Chem. (London)* **1979**, *4*, 1. (c) Silverhorn, W. E. *Adv. Organomet. Chem.* **1975**, *13*, 47.

(2) Orpen, A. G.; Brammer, L.; Allen, F. H.; Kennard, O.; Watson, D. G.; Taylor, R. *J. Chem. Soc., Dalton Trans.* **1989**, Supplement, S1.

(3) Gomez-Sal, M. P.; Johnson, B. F. G.; Lewis, J.; Raithby, P. R.; Wright, A. H. *J. Chem. Soc., Chem. Commun.* **1985**, 1682.

(4) (a) Gallop, M. A.; Gomez-Sal, M. P.; Housecroft, C. E.; Johnson, B. F. G.; Lewis, J.; Owen, S. M.; Raithby, P. R.; Wright, A. H. *J. Am. Chem. Soc.* **1992**, *114*, 2502. (b) Gallop, M. A.; Johnson, B. F. G.; Keeler, J.; Lewis, J.; Heyes, S. J.; Dobson, C. M. *J. Am. Chem. Soc.* **1992**, *114*, 2510. (c) Johnson, B. F. G.; Housecroft, C. E.; Gallop, M. A.; Martinelli, M.; Braga, D.; Grepioni, F. *J. Mol. Catal.* **1992**, *74*, 61. (d) Gallop, M. A.; Johnson, B. F. G.; Lewis, J.; Raithby, P. R. *J. Chem. Soc., Chem. Commun.* **1987**, 1809.

(5) Wadephol, H.; Buchner, K.; Pritzkow, H. *Angew. Chem., Int. Ed. Engl.* **1987**, *26*, 1259.

0276-7333/93/2312-4788$04.00/0

Table I. X-ray Structural Parameters of Known μ_3-η^2:η^2:η^2-Arene Complexes, Taken from Refs 3–5[a]

complex	coord C–C	uncoord C–C	M_3–C_6 angle
$Os_3(CO)_9(\mu_3\text{-}C_6H_6)$	1.41	1.51	1.1
$Ru_3(CO)_9(\mu_3\text{-}C_6H_6)$	1.40	1.45	a few
$Ru_6C(CO)_{11}(\eta^6\text{-}C_6H_6)(\mu_3\text{-}C_6H_6)$	1.39	1.48	0.5
$Os_3(CO)_8(\eta^2\text{-}C_2H_4)(\mu_3\text{-}C_6H_6)$	1.41	1.46	0.8
$Os_3(CO)_8(PH_3)(\mu_3\text{-}C_6H_6)$	1.40	1.43	1.2
$(CpCo)_3(\mu_3\text{-}C_6H_5CH{=}CHMe)$	1.420	1.446	

[a] Distances are given in angstroms, and angles, in degrees.

(μ_3-C_6H_6).[6] This particular coordination mode of benzene (or other arenes) can be compared to the model proposed for chemisorption of benzene in a plane parallel to a solid surface.[1] This point of view, suggested by several experimental studies,[3,4,7] leaves the door open to one of the dreams of chemists, namely modeling surface phenomena through discrete molecular compounds.

X-ray diffraction studies have shown that benzene (or other arenes) adopts the conformation **5**, with three C–C bonds covering the metal centers ("coordinated" C–C bonds) and the other three eclipsing the metal–metal bonds ("uncoordinated" C–C bonds). Another important characteristic of these complexes is that the arene molecule displays a Kekulé-type distortion; C–C bond distance alteration takes place around the C_6 ring, the "coordinated" C–C bonds being shorter than the "uncoordinated" ones. In a localized bond scheme, we can therefore consider the complex as the interaction of a cyclohexatriene with a trimetallic frame (**6**), each double bond interacting with a metal center in a manner similar to the interaction of ethylene with a monometallic fragment. This justifies, with hindsight, the notation used to represent the benzene molecule in the previous drawings. Spectroscopic studies of the C–C stretching modes have effectively shown that the bond alternation is stronger for a μ_3-arene than for a μ_1-η^6 one.[4c] Table I summarizes C–C distances in several μ_3-arene complexes. Even though the trend is consistent with the general one of benzene coordinated on a metallic surface, for which strong distortions are observed,[8] it appears that the Kekulé distortion is sensitive not only to the metal (see the difference between $Os_3(CO)_9(C_6H_6)$ and $Ru_3(CO)_9(C_6H_6)$ in Table I) but also to the nature of the other ligands (see the difference between $Os_3(CO)_9(C_6H_6)$ and $Os_3(CO)_8(\eta^2\text{-}C_2H_4)$). The difference between the two types of C–C distances covers the range 0.03–0.10 Å. One also notices in Table I that the M_3 and the C_6 planes are nearly parallel in all cases.

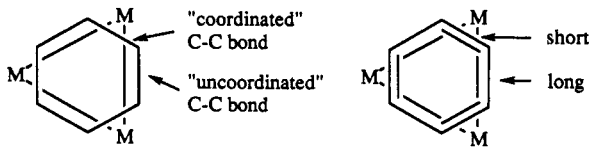

5 **6**

Johnson et al. have investigated through two-dimensional NMR and exchange spectroscopy experiments in solution the fluxionality of the $Os_3(CO)_8(\eta^2\text{-}CH_2CHR)(\eta^6\text{-}C_6H_6)$ complexes for R = H, Me, Ph, *t*-Bu[4] and detected different rearrangement processes: a 1,2-ring-hopping motion exchanging the nuclei in the benzene ligand; a rotation of the olefin around the metal–olefin axis; an exchange between CO and olefin in the $Os(CO)_2$(olefin) species; turnstile rotation in the $Os(CO)_3$ species. Moreover, ^{13}C NMR studies have suggested that the rotation of the C_6 ring and that of the olefin are not coupled. An activation free energy ΔG^* of 11.5 kcal/mol at 211 K has been determined for the rotation of benzene for R = Ph.[4b] Johnson et al. also synthesized the toluene face-capping $Os_3(CO)_8(\eta^2\text{-}CH_2CHR)(\eta^6\text{-}C_6H_5Me)$ (R = H, Ph) complexes. Similar studies led to an activation free energy ΔG^* for the rotation of toluene relative to the osmium triangle at 177 K of around 6.4 kcal/mol for both R = H and R = Ph.[4c] The authors also suggest that similar exchange processes should take place in the solid state. This benzene or toluene rotational barrier is much larger than that for monometallic compounds; for instance, a barrier of 0.5–0.7 kcal/mol has been reported in the case of the η^6 terminal coordination in chromium tricarbonyl complexes (^1H and ^{13}C NMR studies).[9]

In the present paper, we report a theoretical study of the $Os_3(CO)_9(\mu_3\text{-}\eta^2\text{:}\eta^2\text{:}\eta^2\text{-}C_6H_6)$ complex. Our purpose is 2-fold: (a) to determine by *ab initio* molecular orbital (MO) calculations the structure of the complex and (b) to determine the transition state and evaluate and analyze the barrier for rotation of benzene with respect to the Os_3 triangle. Even though this family of compounds has been subject to some theoretical investigations, including calculation of the molecular structure by EH, SCF-Xα, Fenske–Hall methods[4a,10,11] or analysis of photoelectron spectra by MS-Xα methods,[12] as far as we are aware, the present work is the first systematic *ab initio* MO study of trimetallic carbonyl compounds.

Methods of Calculation

The structures of the reactant (the most stable configuration **6**, denoted **A** in the rest of this paper) and also the product, the transition state of the rotational process, and the fragments, $Os_3(CO)_9$ and benzene, have been optimized at the RHF level of theory by an energy gradient method using the Gaussian90 and Gaussian92 packages.[13] Metal centers have been described with

(6) Suzuki, H.; Takaya, Y.; Tada, K.; Kakigano, T.; Igarashi, M.; Tanaka, M. Paper presented at the 39th Symposium on Organometallic Chemistry, Waseda University, Tokyo, Japan, 1992.

(7) (a) Basset, J. M.; Choplin, A. *J. Mol. Catal.* **1983**, *21*, 95. (b) Ertl, G. In *Metal Clusters in Catalysis*; Gates, B. C., Guczi, L., Knozinger, H., Eds.: North-Holland: Amsterdam, 1986. (c) Evans, J. *Chem. Soc. Rev.* **1981**, *10*, 159. (d) Moskovits, M. *Acc. Chem. Res.* **1979**, *12*, 229. (e) Muetterties, E. L.; Rhodin, T. N.; Band, E.; Brucker, C. F.; Pretzer, W. *Chem. Rev.* **1979**, *79*, 91. (f) Muetterties, E. L. *Pure Appl. Chem.* **1978**, *50*, 941.

(8) (a) Lin, R. F.; Blackman, G. S.; Van Hove, M. A.; Somorjai, G. A. *Acta Crystallogr.* **1987**, *B43*, 368. (b) Van Hove, M. A.; Lin, R. F.; Somojai, G. A. *J. Am. Chem. Soc.* **1986**, *108*, 2532.

(9) (a) Jackson, W. R.; Jennings, W. B.; Rennison, S. C.; Spratt, R. *J. Chem. Soc. B* **1969**, 1214. (b) Roques, B. P.; Segard, C.; Combrisson, S.; Wehrli, F. *J. Organomet. Chem.* **1974**, *73*, 327. (c) Albright, T. A.; Hofmann, P.; Hoffmann, R. *J. Am. Chem. Soc.* **1977**, *99*, 7546.

(10) Schilling, B. E. R.; Hoffmann, R. *J. Am. Chem. Soc.* **1979**, *101*, 3456.

(11) (a) Cotton, F. A.; Feng, X. *Inorg. Chem.* **1991**, *30*, 3666. (b) Grieve, G. L.; Hall, M. B. *Inorg. Chem.* **1988**, *27*, 2250. (c) Barreto, R. D.; Fehlner, T. P.; Hsu, L.-Y.; Jan, D.-Y.; Shore, S. G. *Inorg. Chem.* **1986**, *25*, 3572. (d) Halet, J. F.; Saillard, J.-Y.; Lissillour, R.; McGlinchey, M. J.; Jaouen, G. *Inorg. Chem.* **1985**, *24*, 218. (e) Chesky, P. T.; Hall, M. B. *Inorg. Chem.* **1983**, *22*, 2998. (f) Delley, B.; Manning, M. C.; Ellis, D. E.; Berkowitz, J.; Trogler, W. C. *Inorg. Chem.* **1982**, *21*, 2247.

(12) (a) Sham, T. K.; Liu, Z. F.; Tan, K. H. *J. Chem. Phys.* **1991**, *94*, 6250. (b) Sham, T. K.; Liu, Z. F.; Tan, K. H. *J. Chem. Phys.* **1990**, *93*, 4447.

(13) (a) Frish, M. J.; Trucks, G. W.; Head-Gordon, M.; Gill, P. M. W.; Wong, M. W.; Foresman, J. B.; Johnson, B. G.; Schlegel, H. B.; Robb, M. A.; Replogle, E. S.; Gomperts, R.; Andres, J. L.; Raghavachari, K.; Binkley, J. S.; Gonzalez, C.; Martin, R. L.; Fox, D. J.; Defrees, D. J.; Baker, J.; Stewart, J. J. P.; Pople, J. A. *Gaussian92*, Revision A; Gaussian, Inc.: Pittsburgh, PA, 1992. (b) Frish, M. J.; Head-Gordon, M.; Trucks, G. W.; Foresman, J. B.; Schlegel, H. B.; Raghavachari, K.; Robb, M. A.; Binkley, J. S.; Gonzalez, C.; Defrees, D. J.; Fox, D. J.; Whiteside, R. A.; Seeger, R.; Melius, C. F.; Baker, J.; Martin, R. L.; Kahn, L. R.; Stewart, J. J. P.; Topiol, S.; Pople, J. A. *Gaussian90*; Gaussian, Inc.: Pittsburgh, PA, 1990.

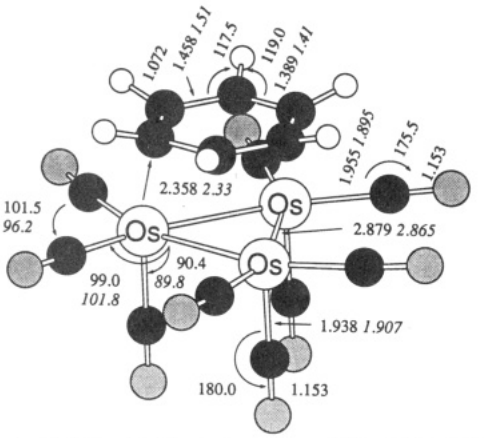

Figure 1. RHF-optimized structure of $Os_3(CO)_9(C_6H_6)$, **A** (C_{3v}). Distances are given in angstroms, and angles, in degrees. Parameters in italics are average experimental values. Other $Os_3(CO)_9$ angular parameters are shown in Table II. The distance between the Os_3 and C_6 ring plane is 2.214 Å (2.19 Å, experimentally).

the relativistic effective core potential of Hay and Wadt, including 60 electrons in the core and a double-ζ-quality basis set for the 16 explicitly treated electrons.[14] The basis set used on the other atoms is a split-valence basis set on benzene (3-21G[15a] on C; 31G[15b] on H) and the minimal STO-3G[15c] on the spectator carbonyl ligands. In order to include the correlation effects for more reliable energetics, we carried out single-point frozen-core Møller–Plesset second-order perturbation (MP2) calculation at the RHF geometry using the previously described basis set.

The extended Hückel (EH) calculations, to be used for a qualitative discussion of the orbitals, have been performed using fixed model geometrical parameters close to the experimental or calculated values. For the $Os(CO)_n$ units (n = 3, 4), we used the following definition: Os–C(CO) = 1.95 Å; C–O = 1.15 Å; CO_{eq}–Os–CO_{eq} = 100°; CO_{eq}–Os–CO_{ap} = 90°. In addition, for polymetallic systems, we have employed an Os–Os distance of 2.85 Å. In all structures, we model the $Os_3(CO)_9$ fragment with equatorial carbonyls (CO_{eq}) in the Os_3 plane. For benzene, a C–C distance of 1.42 Å has been chosen and a local C_{6v} symmetry has been maintained, except for the calculation of **A** and **C** in Figure 7 (local C_{3v} symmetry). The Slater orbitals used for the EH procedure are defined as follows: ζ_s(Os) = 2.450; E_s(Os) = −8.5 eV; ζ_p(Os) = 2.430; E_p(Os) = −3.479 eV; ξ_d = 5.571 (c = 0.6372) + 2.416 (c = 0.5598); E_d = −10.94 eV; ζ_s(C) = 1.625; E_s(C) = −21.4 eV; ζ_p(C) = 1.625; E_s(C) = −11.4 eV; ζ_s(O) = 2.275; E_s(O) = −32.3 eV; ζ_p(O) = 2.275; E_p(O) = −14.8 eV; ζ_s(H) = 1.300; E_s(H) = −13.6 eV.

Ab Initio Calculations: Results and Discussion

Optimization of the Most Stable Configuration. Since the X-ray experiments have shown that the most stable structure is nearly in C_{3v} symmetry with the angle between the Os_3 plane and the C_6 ring plane only 1.1°, we have assumed a C_{3v} constraint in our calculation. This symmetry group requires a planar C_6 ring, equivalent Os–Os distances, and two types of carbonyls: six equatorial ones expected to be nearly in the Os_3 plane and three axial ones expected to be almost perpendicular to it. Figure 1 shows the optimized structure of the most stable configuration **A**. Some additional geometrical parameters are also shown in Table II.

Table II. Main Geometrical Parameters Calculated for the $Os_3(CO)_9$ Unit in Three Complexes: Free Complex, $Os_3(CO)_9(\mu_3\text{-}C_6H_6)$, and $Os_3(CO)_{12}$[a]

param	free $Os_3(CO)_9$ "Os^0"	$Os_3(CO)_9(C_6H_6)$ A	$Os_3(CO)_{12}$
Os–Os	2.794	2.879	2.919
Os–C_{eq}	1.976	1.955	1.963
Os–C_{ap}	1.908	1.938	1.980
C_{ap}–Os–M	97.8	90.5	127.1
C_{eq}–Os–M	126.6	129.1	89.3
C_{eq}–Os–M–D	80.3	85.8	90.0

[a] C_{3v} symmetry is assumed for the two first compounds, and D_{3h}, for $Os_3(CO)_{12}$. Distances are given in angstroms, and angles, in degrees. M is the center of the Os_3 triangle, and D is a dummy atom on the z axis which originates at M and is perpendicular to the Os_3 plane.

Figure 1 indicates that, though the calculated C–C bonds are shorter than the experimental ones, the distortion of benzene is clearly reproduced; the calculated difference of 0.070 Å between the coordinated and uncoordinated C–C bond distances is in reasonable agreement with the experimental value of 0.10 Å. The benzene molecule is globally stretched; the calculated average C–C distance of 1.423 Å (experiment: 1.46 Å) is longer by 0.04 Å (experiment: 0.06 Å) than the free benzene C–C distance of 1.384 Å (experiment: 1.398 Å[1]) calculated at the same level of theory. Since the electron correlation effects are expected to strengthen the interaction between benzene and the metal cluster fragment through the dispersion energy contribution, the geometry optimization at the correlated level will give a larger C–C bond distance alternation and hence a better agreement with the experiment. The C–H bonds are bent away from the C_6 plane at an angle of 18.5°, placing the hydrogen atoms 0.340 Å above the C_6 plane. This is in the range expected experimentally; an estimated value of 0.33 Å from an X-ray diffraction analysis has been proposed for the Ru analog $Ru_3(CO)_9(C_6H_6)$.[4c] The C_{3v} symmetry implies that the C–H bonds need not have the same angle with the short C–C bond and with the long C–C bond; the calculated C–C_{short}–H and C–C_{long}–H angles of 119.0 and 117.5° respectively show that the difference is not very large. The calculated distance between the Os_3 plane and the C_6 ring of 2.214 Å is 0.03 Å longer than the experimental value of 2.19 Å. Again the electron correlation calculation would make the calculated distance shorter.

Concerning the optimized geometry of the Os cluster fragment, the optimized structure **A** is consistent with the general trend obtained in some other triosmium and triruthenium carbonyl complexes.[16] The calculated Os–CO bonds are too long. Such overestimates between 0.05 and 0.10 Å are commonly obtained in HF calculations when carbonyls are involved and have been attributed to the correlation effect.[17] The Os–Os distance of 2.879 Å happens to reproduce the experimental 2.865 Å, but this is not very common. For instance, optimization of complexes such as $Os_3(CO)_{12}$ and $Os_3(CO)_{10}(\mu\text{-L})_2$ has given Os–Os distances too long by 0.05 Å compared to the experimental values, e.g., 2.914 Å calculated vs 2.877 Å experimental[18] in $Os_3(CO)_{12}$. These HF calculations have

(14) Hay, P. J.; Wadt, W. R. *J. Chem. Phys.* **1985**, *82*, 299. In order to minimize the atomic energy and reduce the BSSE, some internal s and p functions have been added to the original set given by Hay and Wadt (5s, 5p, 3d). The employed basis set can be written (4111/4111/21) (Riehl, J.-F. Ph.D. Thesis, University of Paris-Orsay, 1991).

(15) (a) Binkley, J. S.; Pople, J. A.; Hehre, W. J. *J. Am. Chem. Soc.* **1980**, *102*, 939. (b) Hehre, W. J.; Ditchfield, R.; Pople, J. A. *J. Chem. Phys.* **1972**, *56*, 2257. (c) Hehre, W. J.; Stewart, R. F.; Pople, J. A. *J. Chem. Phys.* **1969**, *51*, 2657.

(16) Riehl, J. F.; Koga, N.; Morokuma, K. Unpublished results.

(17) See for instance: (a) Antolovic, D.; Davidson, E. R. *J. Chem. Phys.* **1988**, *88*, 4967. (b) Antolovic, D.; Davidson, E. R. *J. Am. Chem. Soc.* **1987**, *109*, 5828. (c) Dedieu, A.; Sakaki, S.; Strich, A.; Siegbahn, P. E. M. *Chem. Phys. Lett.* **1987**, *133*, 317. (d) Lüthi, H. P.; Siegbahn, P. E. M.; Almlof, J. *J. Phys. Chem.* **1985**, *89*, 2156.

(18) Churchill, M. R.; DeBoer, B. G. *Inorg. Chem.* **1977**, *16*, 878.

shown that improving the basis set to the level of triple-ζ d shell on the metal center and double-ζ basis set on the carbonyls does not improve the results, the calculated bond length changes being only around 0.01 Å.[16]

As shown in Table II, the optimized structure of the $Os_3(CO)_9$ fragment in the benzene complex **A** is qualitatively similar to that of the same fragment in $Os_3(CO)_{12}$. The Os–Os distances are similar in both complexes, 2.865 Å in $Os_3(CO)_9(C_6H_6)$ and 2.877 Å in $Os_3(CO)_{12}$, suggesting a similar nature of bonding. In $Os_3(CO)_{12}$ the apical Os–C bonds *trans* to CO are longer than the equatorial bonds *trans* to Os (1.980 vs 1.963 Å in the calculated structure; 1.946 vs 1.912 Å in the experimental one), suggesting that the *trans* influence of Os is weaker than that of CO. In $Os_3(CO)_9(C_6H_6)$ the calculation and the experiment are at odds concerning the *trans* influence of benzene vs that of Os; the Os–C distance *trans* to benzene vs that *trans* to Os are 1.938 vs 1.955 Å in the calculated structure and 1.907 vs 1.895 Å in the experimental one.

Fragment Optimization. In order to calculate and analyze the interaction energy of benzene with $Os_3(CO)_9$, we have optimized the geometries of the fragments separately. An RHF optimization of benzene gives a C–C distance of 1.384 Å (experiment: 1.398 Å); this structure will be called Bz^0. The structure of benzene in the RHF-optimized complex **A** in Figure 1, on the other hand, will be called Bz^A. The distorted structure Bz^A is higher in energy than the optimized free structure Bz^0 by 23.9 kcal/mol at the RHF level and 15.2 kcal/mol at the MP2 level.

The RHF-optimized structure of free $Os_3(CO)_9$, given in Table II and called Os^0, shows an angular relaxation from that of the $Os_3(CO)_9$ fragment, called Os^A, in the RHF-optimized benzene complex **A**. The relaxation brings the pseudo-C_{3v} axis of the $Os(CO)_3$ unit closer to the Os_3 plane; the angle C_{ap}–Os–M, where M is the center of the Os_3 triangle, of 90.5° in **A** becomes 97.8° in the free species, as seen in Table II. Other significant geometry changes are a shortening of the Os–Os distance from 2.879 to 2.794 Å and of the Os–C_{ap} distance from 1.938 to 1.908 Å, suggesting that the coordination of benzene via its *trans* and *cis* effects induces antibonding factors in the Os–C_{ap} bonds and the Os_3 frame, respectively. This structure seems to correspond to the ground-state equilibrium geometry. At this optimized geometry Os^0, a UHF calculation gives the first triplet state 12.6 kcal/mol higher in energy than the RHF ground state, showing a small triplet–singlet gap. This energy difference may increase at a correlated level, electron correlation stabilizing a closed-shell singlet more than an open-shell triplet. A geometry optimization of the triplet state will, however, decrease the energy gap and might reverse the order, but such a calculation has not been performed.

Compared with the optimized structure Os^0 of $Os_3(CO)_9$, the structure Os^A in the benzene complex **A** is 12.6 kcal/mol at the RHF level and 14.5 kcal/mol at the MP2 level higher in energy. This relatively small energy difference suggests that this fragment is quite flexible and can adjust its geometry substantially to build a stable complex around it.

Interaction Energy. At first we briefly discuss the binding energy of three $Os(CO)_3$ fragments to give $Os_3(CO)_9$. Using the optimized geometry of $Os_3(CO)_9$ and the geometry of $Os(CO)_3$ in $Os_3(CO)_9$, the total cohesive energy ΔE, obtained by $-\Delta E = E(Os_3(CO)_9) - 3E(Os(CO)_3)$, is 261.8 kcal/mol at the RHF level and 349.2 kcal/mol at the MP2 level. Using the optimized geometry of $Os(CO)_3$ (a singlet T-shaped structure), $-\Delta E$ becomes 130.3 kcal/mol (RHF) and 173.7 kcal/mol (MP2). By dividing by 3, one obtains an binding energy of 43.4 kcal/mol at the RHF level and 57.9 kcal/mol at the more reliable MP2 level for each Os–Os bond. The basis set superposition error (BSSE) has to be taken into account for a more accurate estimation of the absolute value of the binding energy. We have not pursued this further, but we can say qualitatively that the Os–Os bond in the cluster complex is strong.

Table III. Benzene Binding Energies (Upper Part) and Rotational Barriers of Benzene (Lower Part) and Their Analysis, Based on Model Intermediate Structures[a]

structure	HF	MP2
$Os^0 + Bz^0$	0.0	0.0
$Os^A + Bz^0$	+12.6	+14.5
$Os^{A*}R^{A*}Bz^0$	−15.5	−116.7
$Os^{A*}R^{A*}Bz^I$	−47.2	−148.5
$Os^{A*}R^{A*}Bz^{II}$	−51.4	−159.2
$Os^{A*}R^{A*}Bz^A$ = A	−54.9	−159.2
$Os^{A*}R^{A*}Bz^{A*}(\theta=0°)$ = A	0.0	0.0
$Os^{A*}R^{A*}Bz^{A*}(\theta=30°)$	+20.1	+24.1
$Os^{A*}R^{A*}Bz^{A*}(\theta=60°)$	+10.8	+4.2
$Os^{B*}R^{B*}Bz^{B*}(\theta=30°)$ = B	+11.3	+26.1
$Os^{C*}R^{C*}Bz^{C*}(\theta=0°)$	+15.7	+10.0
$Os^{C*}R^{C*}Bz^{C*}(\theta=30°)$ = C	+3.4	+15.9
$Os^{A*}R^{A*}Bz^{0*}(\theta=0°)$	+39.4	+42.5
$Os^{A*}R^{A*}Bz^{0*}(\theta=30°)$	+40.9	+51.7

[a] The relative energies are shown in kcal/mol in each part. The energies of Bz^I, Bz^{II}, and Bz^A relative to the optimized Bz^0 are 17.3, 21.8, and 23.9 kcal/mol at the RHF level, respectively, and 14.3, 12.6, and 15.2 kcal/mol at the MP2 level, respectively.

Now we turn our attention to the binding energy between $Os_3(CO)_9$ and benzene to give the benzene complex **A**. As shown in Table III, using the RHF-optimized geometries, one obtains a benzene binding energy of 54.6 kcal/mol at the RHF level and 159.2 kcal/mol at the more reliable MP2 level. The very large difference in the binding energy between the two levels indicates the importance of the correlation energy. Both d-electron-rich metal cluster complex and π-orbital-rich benzene have large polarizabilities, and the dispersion energy contribution should be substantial. The electron correlation is also known to be required to take back-donation into account properly.[19] This large correlation effect is thus expected to affect the geometry of the complex; optimization at the correlated level would make the benzene bond alternation more enhanced and the distance between benzene and $Os_3(CO)_9$ smaller, bringing a better agreement with experiment. However, because of an expected rapid rise of exchange repulsion due to face-to-face contact of electron clouds between benzene and $Os_3(CO)_9$, the latter distance cannot be much smaller.

In evaluating an absolute value of interaction energy, one has to worry about the BSSE, which is not easy to determine.[20] A counterpoise correction (CPC) calculation using ghost basis functions of the respective counterpart at the complex **A** stabilized Os^A and Bz^A by 51.0 (22.3) and 28.8 (11.4) kcal/mol at the MP2 (RHF) level. This

(19) (a) Koga, N.; Jin, S. Q.; Morokuma, K. *J. Am. Chem. Soc.* **1988**, *110*, 3417. (b) Lüthi, H. P.; Siegbahn, P. E. M.; Almlof, J.; Faegri, K.; Jr.; Heiberg, A. *Chem. Phys. Lett.* **1984**, *111*, 1. (c) Moncrieff, D.; Ford, P. C.; Hillier, I. H.; Saunders, V. R. *J. Chem. Soc.* **1983**, 1108.

(20) (a) Sordo, J. A.; Sordo, T. L.; Fernandez, G. M.; Gomperts, R.; Chin, S.; Clementi, e. *J. Chem. Phys.* **1989**, *90*, 6361. (b) Schwenke, D. W.; Truhlar, J. *J. Chem. Phys.* **1985**, *82*, 2418. (c) Schwenke, D. W.; Truhlar, J. *J. Chem. Phys.* **1986**, *84*, 4113. (d) Schwenke, D. W.; Truhlar, J. *J. Chem. Phys.* **1987**, *86*, 3760. (e) Davidson, E. R.; Feller, D. *Chem. Rev.* **1986**, *86*, 681 and references therein.

reduces the total interaction energy from the BSSE uncorrected values of 159.2 (54.6) kcal/mol to 79.4 (20.9) kcal/mol. This kind of CPC calculation has been shown to give a grossly overestimated BSSE, and the true interaction energy should be considered to fall between BSSE uncorrected and present corrected numbers.

Starting from these values of the total interaction energy, we can analyze them further by imagining a model for the benzene approach. Structure **A** can be defined by three sets of parameters: the geometry of $Os_3(CO)_9$ (Os^A), the geometry of benzene (Bz^A), and the distance between the Os_3 and C_6 planes (R^A = 2.214 Å in **A**). We represent the final structure **A** by the notation $Os^A{*}R^A{*}Bz^A$. To build the interaction between $Os_3(CO)_9$ and benzene from the dissociation limit of individually optimized fragments, represented by $Os^0 + Bz^0$, one can imagine the following hypothetical steps: (a) deformation of the $Os_3(CO)_9$ fragment from Os^0 to its geometry Os^A in the complex, (b) formation of a complex of frozen benzene Bz^0 with Os^A at the distance R^A, called the $Os^A{*}R^A{*}Bz^0$ complex, (c) bending of the C–H bonds out of the plane ($Os^A{*}R^A{*}Bz^I$ complex), (d) a global stretch of the C–C bond to the average value in Bz^A ($Os^A{*}R^A{*}Bz^{II}$ complex) and (e) bond alteration of the C_6 ring to finally obtain **A**. The upper half of Table III summarizes the energies of these different structures, relative to the dissociated fragments $Os^0 + Bz^0$. We can observe in this table that at first the deformation of the Os_3 fragments costs only 12–15 kcal/mol, regardless of the method of calculation. The relaxation of benzene from Bz^0 to Bz^A stabilizes the complex by 40–42 kcal/mol, again independent of the methods. If one further analyzes the relaxation of the benzene geometry, one finds that the largest stabilization of 32 kcal/mol is gained by the C–H bending at both the RHF and MP2 levels. Actually this net stabilization of 32 kcal/mol comes at the RHF level from the cost of 15 kcal/mol for changing the benzene geometry from Bz^0 to Bz^I and the gross increase of 47 kcal/mol in the interaction energy. One can see that a low-cost C–H bend causes the π atomic orbitals of benzene to stretch to the outside of the C_6 ring, which in turn provides a more favorable overlap with the metal d orbitals. The global stretch and the bond alternation of the benzene ring add 3 and 4 kcal/mol, respectively, to the net stabilization at the RHF level. These are not very large but are still net gains, and the system takes advantage of all these geometry changes. The MP2 results do not show these relaxation effects clearly, because the structures are not optimized at this level; if optimizations were done at the correlated level, we would see very similar effects.

As discussed above, the electron correlation contribution to the total energy is found to be very large. In the above, however, we have been using the RHF-optimized geometry. In order to assess the effect of geometry changes due to electron correlation, of course, it is most desirable to carry out MP2 optimization. Since this would be too CPU consuming, we have resorted to a "poor man's optimization". We adopted the experimental C=C and C—C distances in the complex of 1.41 and 1.51 Å, respectively; being longer than the RHF-optimized distances, they are likely to be close to the MP2-optimized distances. We also use the experimental Os—C distance of 2.33 Å, corresponding to a distance between the C_6 and Os_3 planes of 2.19 Å, which is shorter than the RHF-optimized value. The Os–Os distances being well reproduced by our calculation and the H atom positions not determined by the X-ray experiment, we employed the RHF-calculated

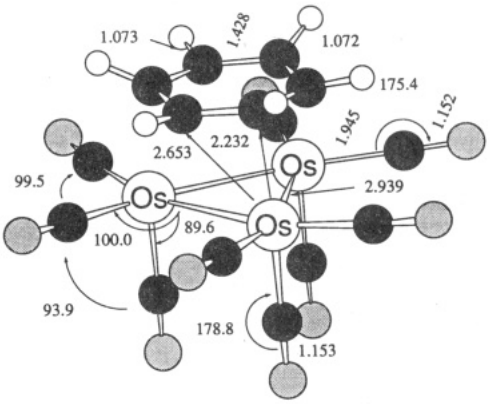

Figure 2. RHF-optimized C_{3v} structure **C** (transition state for internal rotation of benzene) of $Os_3(CO)_9(C_6H_6)$. Distances are given in angstroms, and angles, in degrees.

values for all the other geometrical parameters. An MP2 calculation at this simulated correlated geometry gives a further stabilization energy of 2.0 kcal/mol. This small amount provides a support to our argument that the correlated energy calculated at the RHF geometry gives a good qualitative estimate of its contribution to the true binding energy.

Rotation of Benzene "Rotor". In the transition state for the hindered rotation of the benzene "rotor" in this helicopter complex, the benzene should have three of the six carbon atoms nearly on top of three Os atoms, as shown in **7**. Here all six benzene C–C bonds should be of equal

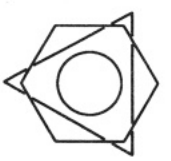

7

length, with overall C_{3v} symmetry for the complex. The transition-state structure, obtained by optimization with C_{3v} symmetry constraint, called structure **C** and denoted as $Os^C{*}R^C{*}Bz^C{*}(\theta = 30°)$ in the notation of Table III, is shown in Figure 2. In this structure, the benzene C atoms do not lie in the same plane, and the C atoms on top of metal atoms are closer to the Os_3 plane than those between two metal atoms, with the deviation out of plane from the average of ±0.040 Å. The average plane of the benzene C atoms is at a distance of 2.178 Å from the Os_3 triangle, which is slightly shorter than 2.214 Å, the calculated distance between the benzene C_6 plane and the Os_3 plane in the equilibrium structure **A**. The C–C distance of 1.424 Å is similar to 1.428 Å, the average of the calculated short and long C–C bond distances (1.389 and 1.458 Å), in **A**. The distances of the carbon atoms from the center of the C_6 ring are 1.447 Å for those on a metal and 1.404 Å for those between two metals, showing a nonnegligible distortion of benzene from hexagonal symmetry. The Os–Os distances have increased to 2.939 Å, 0.060 Å longer than in **A**. These structural changes as one goes from **A** to **C** indicate the rotation of the benzene rotor is far from rigid; both the benzene and the Os_3 fragment intrinsically readjust or relax their structures to minimize the barrier height.

The barrier for rotation of benzene, i.e. the energy difference between the RHF-optimized **C** and **A**, in this complex is 3.4 kcal/mol at the RHF level and 15.9 kcal/

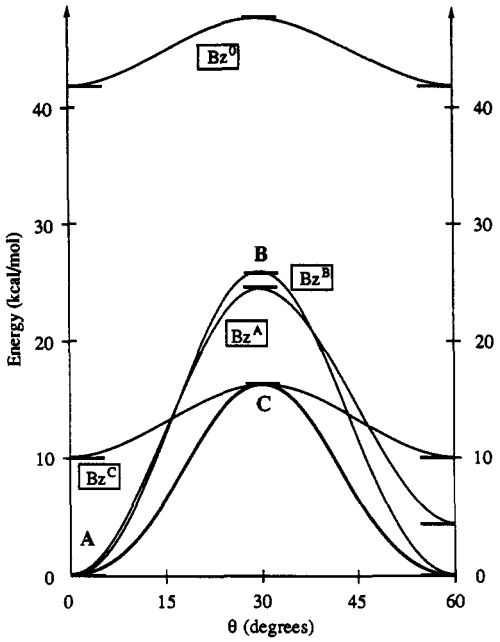

Figure 3. Potential energy profile for rotation (θ) of benzene around the C_3 axis, under various constraints. The thick solid line represents the true barrier. Others represent frozen free benzene (Bz^0), frozen equilibrium geometry (Bz^A), frozen planar benzene (Bz^B), and frozen transition-state (Bz^C) models.

mol at the more reliable MP2 level. A substantial barrier is predicted at the correlated level of calculation. For a more quantitative evaluation of the barrier height, a larger basis set and a better correlation treatment would be required. Though direct comparison with experiment is not possible, our present predicted barrier for rotation of benzene ($\Delta E^{\ddagger}$) of 16 kcal/mol in $Os_3(CO)_9(\eta^6\text{-}C_6H_6)$ may be considered to be in qualitative agreement with an activation free energy ($\Delta G^{\ddagger}$) of 11.5 kcal/mol at 211 K determined for rotation of benzene in $Os_3(CO)_8(\eta^2\text{-}CH_2CHPh)(\eta^6\text{-}C_6H_6)$[4b] and of around 6.4 kcal/mol at 177 K for rotation of toluene in $Os_3(CO)_8(\eta^2\text{-}CH_2CHR)(\eta^6\text{-}C_6H_5Me)$ for both R = H and Ph.[4c]

We wish to analyze this large barrier for benzene rotation. In order to assess the effect of the geometry relaxation of the fragments during the rotation, we have carried out a few series of constrained optimization and frozen geometry model calculations. In the first calculation, we examine the effect of the nonplanar distortion of benzene at the transition state. With the constraint that the six carbon atoms of benzene have to be coplanar with a local C_{6v} symmetry, we have optimized a transition-state geometry. As shown in Table III and Figure 3, using this structure, called **B** or later $Os^{B*}R^{B*}Bz^{B*}(\theta = 30°)$, as the transition state, one obtains a barrier for rotation of 26.1 kcal/mol at the MP2 level with the RHF-optimized geometry, i.e. the MP2//RHF level, about 10 kcal/mol larger than the true barrier (15.9 kcal/mol) based on the fully optimized transition state **C**. Most of this energy difference can be attributed to the relaxation of benzene, and the relaxation of the trimetallic fragment accounts for less than 1 kcal/mol. In the succeeding models, therefore, we pay attention mainly to the geometry of benzene. The ability of the circular "chain" of benzene carbon atoms to move up and down individually, depending on the "shape" of the Os cluster base, apparently plays an important role in making the rotation not too difficult.

In the second series, we assumed that the fragment geometries at the equilibrium geometry **A** are frozen and let benzene make a "rigid" rotation around the vertical axis through the centers of the Os_3 and C_6 rings. This angle of rotation will be denoted θ, the origin being taken at **A** ($\theta = 0°$). With the addition of this degree of freedom, the complex is now defined by four parameters, **A** being written $Os^{A*}R^{A*}Bz^A(\theta = 0°)$. This "rigid" rotation mechanism leads to a transition state of C_1 symmetry in the vicinity of $Os^{A*}R^{A*}Bz^A(\theta = 30°)$, **8**, and a local minimum,

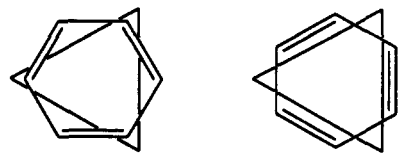

8 **9**

$Os^{A*}R^{A*}Bz^A(\theta = 60°)$, **9**, with "wrong" C–C bonds coordinating, i.e. with coordinated C–C distances longer than uncoordinated ones. The results are shown in Table III and Figure 3. The barrier would be 24.1 kcal/mol, about 8 kcal/mol higher than the true barrier, indicating that the bond alternation is very unfavorable at the transition state. The structure **9** is less stable than the true minimum **A** by about 4 kcal/mol, suggesting that the interaction of longer, wrong C–C bonds is costly even at the bottom of the barrier.

In the third series, we froze the fragment geometries at the transition state **C**. As shown in Table III and Figure 3, the stable conformation ($\theta = 0°$) is destabilized by 10 kcal/mol, relative to the absolute minimum **A**. The lack of bond alternation in Bz^C makes the interaction less favorable for $Os^{C*}R^{C*}Bz^C(\theta = 0°)$. In the last series, we let the free benzene molecule Bz^0 interact with the Os^A fragment without relaxation and rotate rigidly. As discussed before, the binding is much weaker here (−42 kcal/mol), but the rotational barrier is lowered (around 2 kcal/mol at the RHF level and 9 kcal/mol at the MP2 level).

Comparison with a Mononuclear Ethylene Complex, $W(CO)_5(C_2H_4)$. Our calculations of $Os_3(CO)_9(\mu_3\text{-}C_6H_6)$ have shown that the interaction energy increased drastically by taking into account the effect of electron correlation. As the interaction of benzene with $Os_3(CO)_9$ can be considered formally as a coordination of three double bonds to three metallic centers, it is interesting to compare the present system with the interaction of ethylene with a monometallic fragment in the same electronic environment. It is well-known that the π complex formed with ethylene and a metal of the third transition row is a very stable species with an interaction energy of up to 50 kcal/mol,[21] which is close to one-third of the triene interaction energy obtained in the $Os_3(CO)_9(\mu_3\text{-}C_6H_6)$ calculations (159 kcal/mol). Here we wish to make a direct comparison between a mononuclear ethylene complex and the trinuclear benzene complex using the same type of basis set and the same calculation methodology. For a mononuclear system, geometry optimization at the MP2 level is feasible, and thus we will be able to assess the effect of geometry changes due to electron correlation.

The most natural way to make this comparison would be the interaction of an ethylene molecule with $Os(CO)_5$ in a square pyramidal (SP) geometry, which would place

(21) Koga, N.; Morokuma, K. *Chem. Rev.* **1991**, *91*, 823.

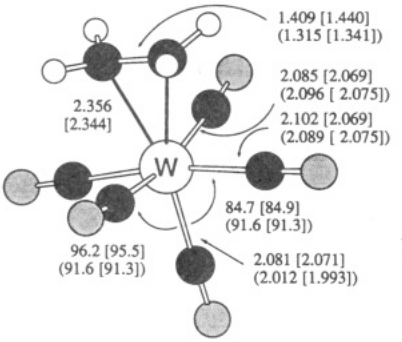

Figure 4. RHF- and MP2-optimized (square brackets) structures of $W(CO)_5(C_2H_4)$ (C_{2v} assumed). Distances are given in angstroms, and angles, in degrees. The parameters of the $W(CO)_5$ (C_{4v}) and C_2H_4 (D_{2h}) fragments are given in parentheses.

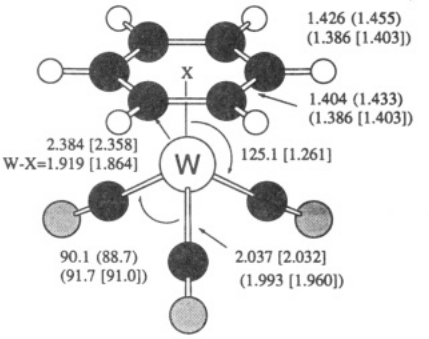

Figure 5. RHF- and MP2-optimized (square brackets) structures of the staggered conformation of $W(CO)_3(\eta^6\text{-}C_6H_6)$ (C_{3v} assumed). Distances are given in angstroms, and angles, in degrees. The parameters of the $W(CO)_3$ (C_{3v}) and benzene (D_{6h}) fragments are given in parentheses.

the osmium metal atom in the same electronic configuration (d^8) as that in $Os_3(CO)_9$ and in a ligand field similar to that in $Os_3(CO)_9$. This model unfortunately does not work. The optimal structure of a d^8 ML_5 complex is a trigonal bipyramid (TBP), and even if we force the $Os(CO)_5$ fragment to have a SP geometry, no acceptor orbital is available except for an sp hybrid which is high in energy and not convenient for a strong interaction. Since it is preferable to use a neutral zerovalent metal with a carbonyl ligand field, a natural choice is a complex of SP d^6 $W(CO)_5$ with C_2H_4.[22]

Figure 4 shows the structure of $W(CO)_5(C_2H_4)$, optimized under C_{2v} constraint at the both RHF and MP2 levels. This structure is the most stable structure. (The other C_{2v} structure in which the ethylene is staggered with all four carbonyl ligands, making them equivalent, is higher in energy by 4.0 kcal/mol, because of a smaller back-donation; this structure is in fact the transition state of the rotation process of ethylene around an axis crossing W and the middle of the C=C bond.) Going from the RHF to the MP2 geometry, the main observable changes are a shortening of the W—CO distances and a lengthening of the C=C bond from 1.409 to 1.440 Å, both longer by about 0.09 Å than that in free ethylene. One notices that, if the RHF → MP2 C=C distance change is added to the RHF-optimized C—C_{short} distance of the benzene complex in Figure 1, one obtains 1.42 Å, which is in quite good agreement with experiment, 1.41 Å. This suggests that MP2 optimization of $Os_3(CO)_9(\mu_3\text{-}C_6H_6)$ will probably give a good geometry. The W—$C_{ethylene}$ distance changes only by 0.012 Å, supporting the argument made previously that the M—benzene distance cannot become much shorter upon inclusion of electron correlation.

The binding energy, the energy of respectively optimized fragments relative to that of the product complex, is 27.4 kcal/mol at the RHF level and 53.1 kcal/mol at the MP2//MP2 level, with the MP2//RHF energy of 50.8 kcal/mol. As in the case of trinuclear benzene complex, one has to consider the BSSE. A CPC calculation using ghost basis functions stabilized $Os(CO)_5$ and ethylene by 17.9 (6.9) and 8.6 (5.9) kcal/mol at the MP2 (RHF) level, respectively. These values reduce the BSSE uncorrected interaction energy of 53.1 (27.4) kcal/mol to 26.6 (14.6) kcal/mol. As discussed before, the CPC is expected to overestimate the BSSE and the true bonding energy will fall between the two values, in the range 30–50 kcal/mol at the more reliable MP2 level. One should notice the good proportionality between the mono- and the trimetallic compounds; the uncorrected interaction energy, the CPC energy, and thus the corrected interaction energy in $W(CO)_5$ are very close to one-third of the values calculated for $Os_3(CO)_9$(benzene).

Comparison with the Mononuclear Benzene Complex $W(CO)_3(\eta^6\text{-}C_6H_6)$. Another point of comparison is the energy of the interaction of benzene with a monometallic fragment; a d^6 ML_3 fragment can serve as a model monometallic fragment. If we want to use carbonyl ligands and a third-row transition metal, a natural choice is $W(CO)_3(C_6H_6)$. The series $M(CO)_3$(arene), M=Cr, Mo, W, has been studied for various arenes. Experimentally, both staggered and eclipsed structures have been observed, depending of the nature of the metal and of the arene ligand. For instance, $Cr(CO)_3(C_6H_6)$ is known to adopt the staggered conformation, while $Cr(CO)_3(C_6Et_6)$ is found in the eclipsed one.[1]

Figure 5 shows the RHF- and MP2-optimized structures of $W(CO)_3(C_6H_6)$ in the staggered conformation. As expected from our discussion in a preceding subsection, benzene C–C bonds in the complex are more stretched (+0.042 Å) in the MP2 structure than in the RHF one, relative to those in free benzene. The MP2 average benzene C–C distance of 1.444 Å may be compared with the experimental value of 1.415 Å in $Cr(CO)_3(C_6H_6)$[23a] and 1.423 Å in $Mo(CO)_3(C_6(CH_3)_6)$.[23b] The RHF W–C distance of 2.384 Å is similar to the distances in **A** (calc = 2.358 Å; exp = 2.33 Å). In this mononuclear case, shorter C–C bonds are *trans* to the carbonyl ligands. Therefore, if benzene coordinates to W with the shorter bonds, this complex is an octahedral complex. If the coordination is made with the longer bonds, the complex is similar to a prismane, which is an unstable structure. One can therefore conclude that, as in the trimetallic case, coordination of benzene takes place through the shorter bonds, suggesting that this mode of coordination is an intrinsic property of benzene complexes. For the shorter bonds, occupied π orbitals are an in-phase combination and π^* orbitals, an out-of-phase combination, which is appropriate for a strong complexation. At the longer bonds, the phase relation is opposite and thus not appropriate for complexation.

(22) For this complex, we used the same type of basis sets as for $Os_3(CO)_9(C_6H_6)$: the relativistic effective core potential of Hay and Wadt with 60 electrons in the core, associated with a double-ζ basis set on W, minimal STO-3G basis set on the spectator carbonyl ligands, split-valence basis set on C_2H_4 (3-21G on C; 6-31G on H). A reoptimized basis set being unavailable for W, we employed the original set of primitives given by Hay and Wadt.[14]

(23) (a) Rees, B.; Coppens, P. *Acta Crystallogr.* **1973**, *B29*, 2516. (b) Koshland, D. E.; Myers, S. E.; Chesick, J. P. *Acta Crystallogr.* **1977**, *B33*, 2013.

We also have determined the eclipsed conformation, which should give an estimation of the rotational barrier of benzene. Compared to the staggered conformation, this structure is less stable by 0.2 kcal/mol at the RHF level but more stable by 0.1 kcal/mol at the MP2//MP2 one. Even though more accurate calculations with a larger basis set would be necessary to determine the most stable structure, this calculation clearly indicates that the rotation of benzene in this monometallic complex is essentially free, much easier than in the trimetallic compounds (15.9 kcal/mol calculated at the MP2//RHF level for the trimetallic complex $Os_3(CO)_9(C_6H_6)$).

The binding energy of benzene, the difference in total energy between $W(CO)_3(C_6H_6)$ in the staggered conformation and individually optimized fragments (we used for $W(CO)_3$ the energy of the optimized singlet C_{3v} structure, which seems to be the global minimum, the singlet or triplet C_{2v} T-shaped structures being higher in energy), is 64.4 kcal/mol at the RHF level and 112.3 kcal/mol at the MP2//MP2 level (113.6 kcal/mol at the MP2//RHF level). A CPC calculation stabilizes $Os(CO)_3$ and benzene by 28.1 (8.7) and 20.5 (14.6) kcal/mol at the MP2 (RHF) level. Thus the MP2 binding energy with the CPC is 65 kcal/mol, giving a range for the binding energy of 65–110 kcal/mol. This can be compared with the above estimated range of the benzene binding energy of 80–160 kcal/mol for $Os_3(CO)_9(C_6H_6)$. This result shows that the benzene has a slightly weaker but nearly strong interaction with a monometallic fragment as compared with a trimetallic fragment.

Orbital Analysis of the Electronic Structure of $Os_3(CO)_9(C_6H_6)$

$Os_3(CO)_9$ Fragment. In order to gain some insight into the qualitative nature of the electronic structure of $Os_3(CO)_9$(benzene), as well as the origin of the high rotational barrier, we have built orbital correlation diagrams based on EH calculations. EH MOs are usually easier to analyze than *ab initio* MOs because of the smaller number of "basis functions" involved. Moreover, interactions are clearly visualized, being directly proportional to the atomic overlaps.

At first, we briefly describe the electronic structure of the $Os_3(CO)_9$ fragment, already detailed by Hoffmann and Schilling,[10] as well as by Barreto et al.[11c] The orbital correlation diagram of $Os_3(CO)_9$ built from three $Os(CO)_3$ units is shown on Figure 6. The valence d MOs of C_{2v} $Os(CO)_3$ consist of three low-lying t_{2g}-like orbitals (1a″, 1a′, and 2a′) and higher orbitals 2a″ and 3a′. In neutral $Os(CO)_3$, the orbitals are filled up to 2a″. The interaction of three $Os(CO)_3$ units converts the t_{2g}-like orbitals into a set of nine low-lying nearly degenerate occupied orbitals, which are essentially d lone pairs on the metals and contribute little to the Os–Os bond. The 2a″ orbitals lead to the 4e occupied Os–Os σ-bonding orbitals and the vacant $2a_2$ orbital. The 3a′ orbitals lead to the occupied $3a_1$ orbital and the vacant orbitals 5e. These three occupied orbitals mainly contribute to the σ Os–Os bonds. Because of these strong σ Os–Os bonds, $Os_3(CO)_9$ should have a good intrinsic stability but at the same time should behave as an excellent electron donor and acceptor. In addition, the $Os(CO)_3$ sp hybrid 4a′ is strongly stabilized to give a supplementary low-lying orbital ($4a_1$), correctly set up to have a good interaction with a capping ligand.

This case is quite different from what is expected in a monometallic fragment having the same metal characteristics. The d^8 ML_5 complex with a square pyramid-like ligand field has no d acceptor orbital; the first accessible vacant orbital is an sp hybrid, often too high in energy to give a good interaction. Actually the most stable structure for a d^8 ML_5 complex is a D_{3h} trigonal bipyramid. These considerations justify, with hindsight, why the interaction of benzene with an $Os_3(CO)_9$ fragment can be compared, as we did in a preceding section, with the interaction of ethylene with a d^6 ML_5 fragment; both fragments formally have one acceptor and one donor orbital on each metal and essentially retain their original stable geometries after interaction.

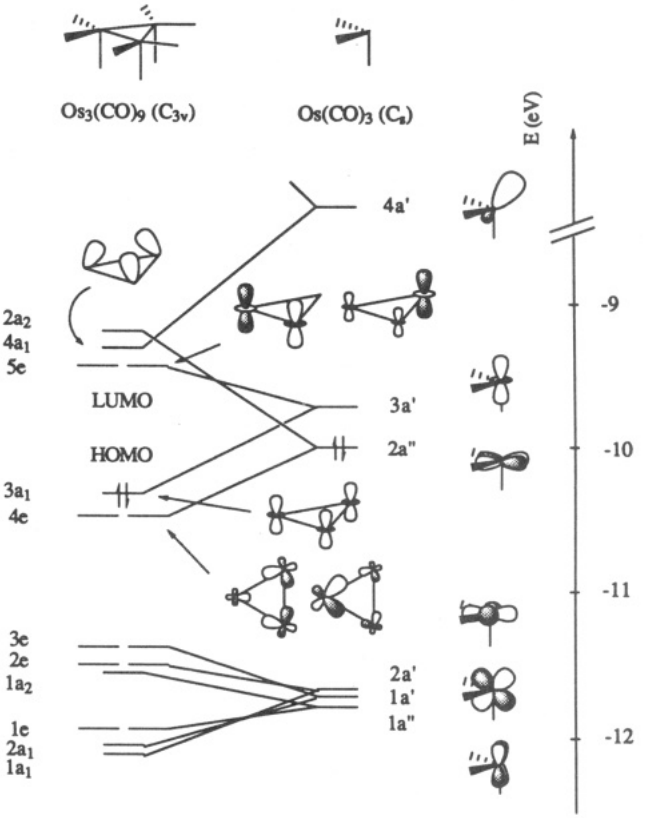

Figure 6. Orbital correlation diagram of $Os_3(CO)_9$ built from three $Os(CO)_3$ units. For clarity, carbonyl contributions are not shown.

Interaction with Benzene. Figure 7 shows the evolution of the d orbitals of the $Os_3(CO)_9$(benzene) complex in various geometries, starting from the orbitals of $Os_3(CO)_9$ (first column) and benzene (last column). For the benzene complex, we have maintained the MO labels for $Os_3(CO)_9$ and benzene fragments for easier identification. First, we look at the second column, which shows the energy levels after interaction of Os^A with a free benzene (Bz^0). Looking at this diagram, we can easily find that the low-lying t_{2g}-like d lone-pair orbitals, $1a_1$ to 3e, in $Os_3(CO)_9$ do not participate strongly in the primary interaction with benzene. Compared to their level in the free $Os_3(CO)_9$ fragment, they are slightly destabilized because of the so-called four-electron or exchange repulsion with the occupied σ and π orbitals of benzene. The donative interaction, shown by bold lines in Figure 7, mainly takes place between the HOMOs, the e_{1g} π orbitals, of benzene and LUMOs (5e) of $Os_3(CO)_9$. As shown in Figure 6, the $Os_3(CO)_9$ 5e MOs consist mainly of metal d_{z^2} orbitals and are very suitable for interaction with benzene π orbitals. The back-donation, shown by thick dashed lines in Figure 7, mainly occurs between the next HOMOs (4e) of $Os_3(CO)_9$ and the e_{2u} π^* orbitals of benzene to give

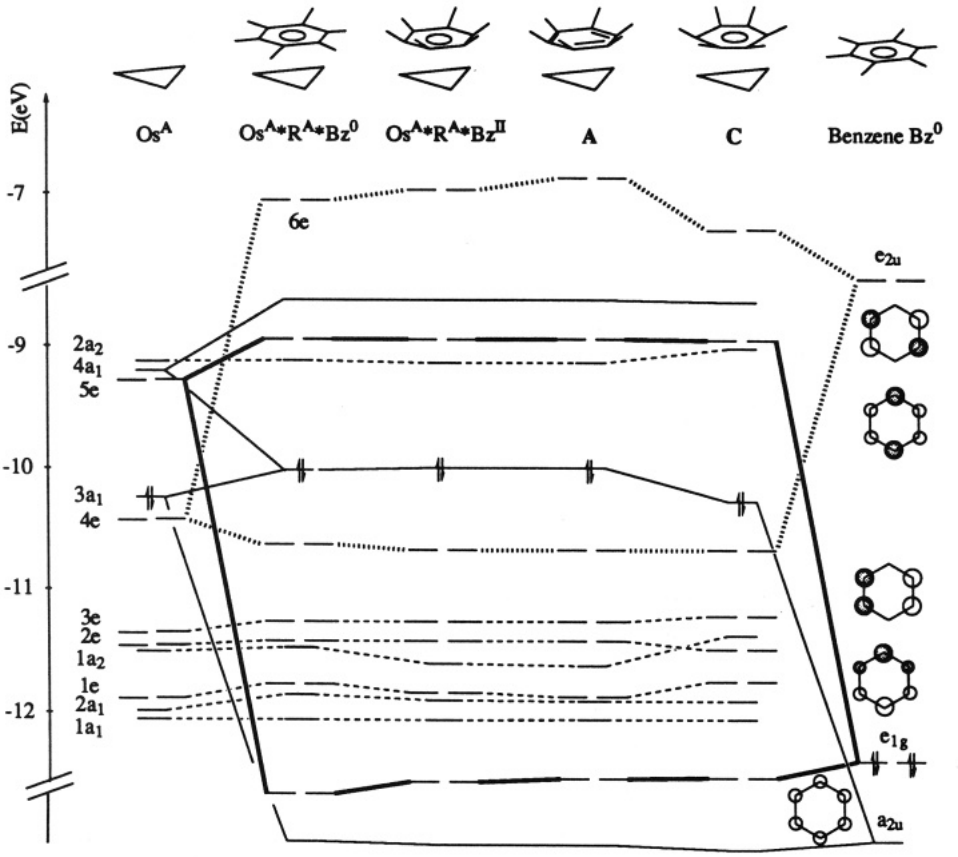

Figure 7. Orbital correlation diagram for interaction between $Os_3(CO)_9$ and benzene. Solid bold lines denote donative interactions, dashed bold lines, back-donative interactions, and the thin solid lines, interactions among a_1 symmetry. Orbitals with a double arrow are the HOMOs.

the 4e occupied and the 6e vacant orbitals. As discussed and shown also in Figure 6, the $Os_3(CO)_9$ 4e MOs are Os–Os σ bonding and localized mostly in the Os_3 plane and, therefore, not most suited for a good interaction with benzene. However, metal d orbitals are polarized in the direction of the middle of Os_3 triangle by metal p orbitals and rotated in the direction of benzene by a contribution of xz and yz orbitals. Moreover, C p_z orbitals point to the direction of the in-plane d lobes, e.g., xy lobes for the metal localized on the x axis. The overlap and the interaction between these orbitals can thus be strong. Such a scheme has already been suggested by Schilling and Hoffmann[10] and Halet et al.[11d] in their EH study of the interaction of acetylene with a trimetallic cluster and by Johnson et al. for the $Ru_3(CO)_9(C_6H_6)$ model complex (Fenske–Hall calculations).[4a] Finally, the $Os_3(CO)_9$ HOMO ($3a_1$) is destabilized by the exchange repulsion with the symmetric benzene π orbital (a_{2u}); mixing of an extra low-lying vacant sp hybrid ($4a_1$) orbital with this interaction, however, will contribute to the restabilization of the system (solid line in Figure 7).

In the real complex, the benzene molecule becomes nonplanar, as seen in our *ab initio* optimized structure, where the C–H bonds are bent out of the C_6 plane by 18.5°. The energy levels obtained when the C–H bonds are bent out of the C_6 plane are shown in the third column of Figure 7 ($Os^{A*}R^{A*}Bz^{II}$ compound). In a free benzene molecule, such a distortion raises the energies of the occupied π orbitals, thus destabilizing benzene, and lowers those of the vacant π^* orbitals by a mixing with σ_{C-C} antibonding orbitals. This mixing and resultant redirectioning of the π^* orbitals toward the outside of the benzene ring increase the overlap with the d orbitals of the $Os_3(CO)_9$ fragment. The resulting strengthening of the interactions is visualized by a slight stabilization of the metal-based donor 4e orbitals.

A very important stabilization comes from 1e and $1a_2$ orbitals, which do not primarily participate in the bonding interaction. The destabilization of these orbitals in the column 2 of Figure 7 for planar benzene is substantially reduced when the C–H bonds are bent. The 1e (**10**) and

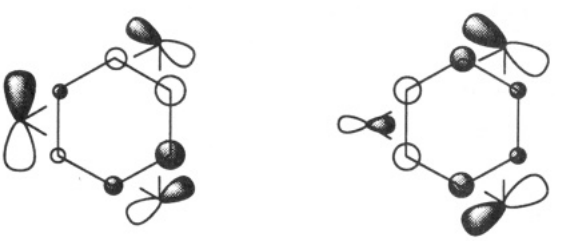

a b

10 (1e)

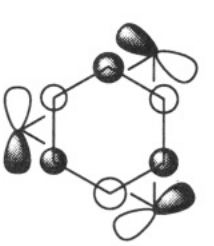

11 ($1a_2$)

$1a_2$ (**11**) are Os–C bonding.[24] The $1a_2$ orbital of $Os_3(CO)_9$ can interact more strongly with the benzene b_{2g} π^* orbital when benzene is bent, contributing to a larger back-

donative attraction. The same can be said for the interaction between the 1e orbitals of $Os_3(CO)_9$ (**14**) and the e_{2u} π^* orbitals of benzene. When benzene is bent, the 1e and $1a_2$ electrons can also avoid exchange repulsion from the occupied benzene σ_{C-H}. Though individual energy changes may not be very large, the global effect involving six electrons could be substantial.

Origin of the Benzene Kekulé Distortion. In this paragraph, we give an orbital interpretation of the C_6 ring Kekulé distortion and try to understand how the bond alternation around the C_6 ring makes the interaction with $Os_3(CO)_9$ stronger. At first, we recognize that the EH overlap populations (OP) are consistent with this C–C bond alternation. Using equivalent C–C distances, the OP of the coordinated C–C bonds is larger than the OP of the uncoordinated C–C bonds (1.003 vs 0.968). These two OPs are still smaller than the OP in a free molecule calculated with the same C–C distances (1.064), again consistent with the global stretch of benzene after interaction with $Os_3(CO)_9$.

As shown before, the Kekulé distortion of the present magnitude destabilizes the benzene molecule by 2–3 kcal/mol. Therefore, upon distortion, there must be an increase in the net attractive interaction that is larger in magnitude than the benzene distortion energy. Here we will illustrate this in terms of mixing of π and π^* orbitals and their interaction with metal d orbitals.

Under C_{3v} symmetry, the mixing of the e_{1g} (**12**) π and e_{2u} (**13**) π^* orbitals becomes allowed. Though this mixing stabilizes the π-electronic energy of benzene, it is not sufficient to cause the Kekulé distortion.[25] We must consider their interaction with appropriate $Os_3(CO)_9$ orbitals, in this case, with the midenergy 1e orbitals of $Os_3(CO)_9$ (**14**). Since the set of the three orbitals designated by **b** within each degenerate pair gives the same interaction scheme as the set designated by **a**, we will concentrate our discussion on **a** orbitals. With our sign convention, the overlap between **12a** and **14a** and that between **13a** and **14a** are positive. The lowest occupied EH MO **15a** resulting from the interaction consists mainly of **12a** with a positive small mix of **13a** and **14a**. We can write this MO as **15a** = **12a** + λ**14a** + μ**13a**, where λ and μ are small positive mixing coefficients which are nonzero and zero, respectively, when Kekulé distortion is not present. The change of this MO energy upon Kekulé distortion is of the order $\lambda\mu\langle$**13a**$|h|$**14a**$\rangle$, which is of the second order and is thus small, as seen in Figure 7.

One can see in Figure 7 that the most important stabilization upon Kekulé distortion comes from the second occupied orbital, already shown as **10a**, which consists mainly of the metallic d orbital **14a**, with a mixing of **12a** and **13a** in the mutually opposite sign, in the present convention, a positive mix of π^* and a negative mix of π. We can write this orbital as **10a** = **14a** − λ'**12a** + μ'**13a**, where λ' and μ' are positive mixing coefficients. In this three-orbital model, the energy level variation of the energy level of **10a** relative to **14a** can be written at the first order

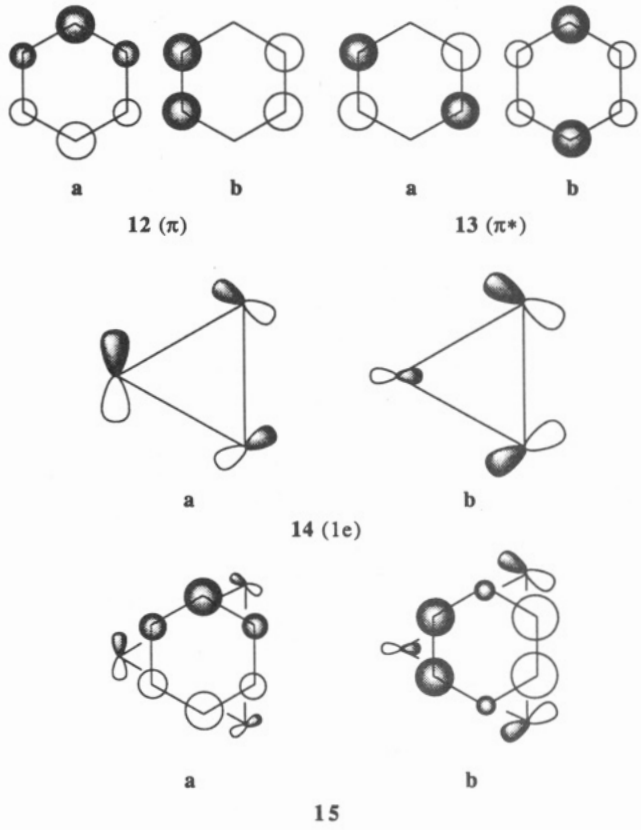

as

$$\Delta E = -2\lambda'\langle \mathbf{12a}|h|\mathbf{14a}\rangle + 2\mu'\langle \mathbf{13a}|h|\mathbf{14a}\rangle$$

The change in energy upon Kekulé distortion is therefore expressed as

$$\Delta\Delta E = \Delta E(\text{distorted}) - \Delta E(\text{undistorted})$$

Since ΔE is expressed as a difference of two negative numbers, the sense of variation of $\Delta\Delta E$ depends on the variation of the resonance integrals $\langle$**12a**$|h|$**14a**$\rangle$ and $\langle$**13a**$|h|$**14a**$\rangle$, which are proportional to the overlaps $\langle$**12a**|**14a**$\rangle$ and $\langle$**13a**|**14a**$\rangle$, as well as on the coefficients λ' and μ'. An analysis of the overlaps between fragment orbitals shows that, upon Kekulé distortion, the d–π overlaps are decreased while the d–π^* overlaps are increased; the d–π overlap $\langle$**12a**|**14a**$\rangle$ of 0.058 in the undistorted structure becomes 0.052 after distortion, and the d–π^* overlap $\langle$**13a**|**14a**$\rangle$ of 0.088 in the undistorted structure becomes 0.092 after distortion. These changes are quite reasonable. The benzene π MO **12a** will gain a bonding character in the shortened bonds upon distortion, which will decrease the overlap with **14a**, which is antisymmetric with respect to these bonds; the benzene π^* MO **13a** will gain an antibonding character in the shortened bonds upon distortion, which will increase the overlap with **14a**. The changes in the overlap is of course transferred to the coefficients λ' and μ'; λ' is diminished upon distortion, while μ' is increased. Overall, both the increase in the magnitude of the $2\mu'\langle$**13a**$|h|$**14a**$\rangle$ term, which represents the back-donation, and the decrease in the magnitude of the $-2\lambda'\langle$**12a**$|h|$**14a**$\rangle$ term, representing the exchange repulsion, operate in the same direction and make $\Delta\Delta E$ very negative. In other words, the system is stabilized upon distortion both by an increase in back-donation and by a decrease in exchange repulsion.

Figure 7 also shows some stabilization of the $1a_2$ orbital upon Kekulé distortion. As shown before, this orbital **11** is strongly back-donative and the interaction is enhanced

(24) For clarity, we will represent, in the following diagrams, the d orbitals other than xy and $x^2 - y^2$ by p-like orbitals, omitting the part which does not point in the direction of benzene ($z < 0$); the z^2 orbitals will be represented by sp hybrid orbitals and benzene π orbitals by s orbitals, omitting the part which does not point in the direction of the Os_3 plane.

(25) Shaik, S. S.; Hiberty, P. C.; Ohanessian, G.; Lefour, J.-M. *J. Phys. Chem.* **1988**, *92*, 5086.

due to more favorable overlap upon Kekulé distortion; considering the interaction of the $Os_3(CO)_9$ $1a_2$ orbital with the benzene a_{2u} and b_{2g} orbitals leads to the same argument that we discussed in the previous paragraphs for **12–14**. Though we have not determined the relative weight of these factors in favor of Kekulé distortion, the EH MO energy changes and our analysis above suggest that most important contribution comes from **10a,b** followed by that of **11**.

Origin of the Rotational Barrier of Benzene. The last point we wish to examine is the origin of the rotational barrier of benzene. The fifth column of Figure 7 shows the EH MO levels in the rotational transition state **C**. Compared to the energy levels in **A** (column 4), four occupied orbital sets are affected by the rotation of benzene: the two degenerate sets 1e and 2e, $1a_2$, and the HOMO $3a_1$. The orbitals 1e and $1a_2$, the same ones which were stabilized by the C–H bend, are destabilized, while 2e and $3a_1$ are stabilized.

Let us examine first the case of $3a_1$. In **A**, this orbital is destabilized by a four-electron repulsion with the full symmetric a_{1g} π orbital of benzene and the σ_{C-C} orbitals having the same symmetry, leading to the orbital illustrated in **16**. In **C**, this mixing is still allowed, but an

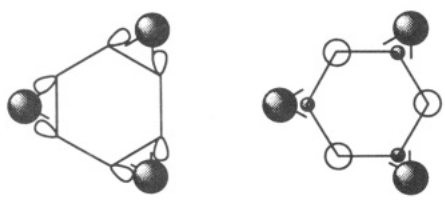

16 ($3a_1$) **17** ($3a_1$)

interaction with the b_{2g} π^* orbital is now possible (**17**), leading to a large stabilization of the HOMO and an increased Os–C bonding character, C eclipsing the metal centers, consistent with shorter Os–C distances calculated for **C** with the *ab initio* method. The 2e orbitals are mainly built from $Os(CO)_3$ 2a′ orbitals and could not interact with benzene in **A**. In the rotated structure **C**, the mixing of 2e with the benzene π and π^* orbitals becomes possible. The total stabilizing interaction results from the larger overlap with π^*, which has a larger spatial extension than the π orbitals. The stabilization is however small, the 2e $Os_3(CO)_9$ orbitals mainly lying in the metal plane.

We now turn our attention to the destabilizing contributions from 1e and $1a_2$, which should be the decisive factors. For these three orbitals, respectively represented in **10** and **11**, the stabilizing interaction with π^* allowed in **A** is forbidden after a 30° rotation of benzene, with the carbon p orbitals pointing to the nodal plane of the metal d orbitals. Actually, one of these π^* orbitals is used for mixing with $3a_1$ in **C**, as discussed above with **17**. This destabilization is enhanced further by exchange repulsion with σ_{C-C} orbitals, which cannot be compensated by a interaction with the very high lying σ^*_{C-C} orbitals. The result is a net destabilization of these orbitals. The orbital $1a_2$ (**11**) and the component **10a** of the 1e orbitals after rotation of benzene are shown in **18** and **19**, respectively. It can be seen from these drawings that the Os–C binding contributions of these orbitals in **A** are lost in **C**.

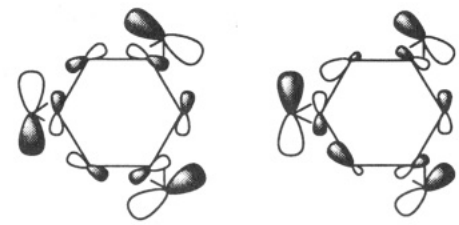

18 ($1a_2$) **19** (1e)

The system is destabilized by the rotation of benzene as a result of all these factors combined. Apparently, the destabilization of six electrons by the loss of d–π^* interactions and the appearance of exchange repulsion between the metal d electrons and the σ_{C-C} electrons cannot be compensated by the stabilization of the two HOMO and the four 2e electrons, leaving a relatively high barrier.

Conclusions

The present *ab initio* calculation and MO analysis have clarified the nature of the interaction of benzene with the $Os_3(CO)_9$ fragment and the origin of the rotational barrier. This interaction follows the traditional donation/back-donation scheme, but in contrast to the case of mononuclear complexes, the back-donation takes place through metal orbitals localized in the metallic plane which behaves as an electron-reservoir. The benzene molecule becomes non-planar to maximize the stabilization, mainly to reduce the exchange repulsion between the d electrons and the benzene π electrons. Moreover, the benzene ligand undergoes a Kekulé distortion to further stabilize the system, by enhancing back-donative interaction and reducing exchange repulsion.

The rotational barrier found for benzene, much stronger than that for the μ_1-η^6 coordination, is the result of loss in the back-donative interaction and increase in the exchange repulsion in the rotated structure. This case is quite different from the case of, for instance, ML_3–arene species, for which the delocalization of the π orbitals around one metal center can assume a constant back-donation and for which the four-electron destabilization does not exist, the σ_{C-C} and σ_{C-H} orbitals being unable to mix with the metal orbitals.

From a methodological point of view, these calculations have shown that RHF optimizations provide sufficient structural accuracy to allow a discussion of the properties of this cluster. This behavior is however limited to the third transition metal row (and also the second row, even though accuracy would be lower).

Acknowledgment. Numerical calculations were partly carried out at the Computer Center of the IMS. J.-F.R. acknowledges the Japan Society for Promotion of Science for his postdoctoral fellowship. The present research was in part supported by a Grant-in-Aid for Scientific Research in the Priority Area of "Theory of Chemical Reactions" from the Ministry of Education, Science, and Culture of Japan.

OM930450I